

Jens Marquetand, Uwe Riedel:

A Two-equation Model to Simulate Soot Formation under Shock-tube Conditions

Zeitschrift für Physikalische Chemie 223 (2009), 605-619.

This paper was published in "Zeitschrift für Physikalische Chemie" and is made available as an electronic reprint with the permission of Oldenbourg Wissenschaftsverlag.

**A two-equation model to simulate soot formation
under shock-tube conditions**

Dipl.-Ing. Jens Marquetand: Interdisziplinäres Zentrum für Wissenschaftliches Rechnen (IWR), Universität Heidelberg, Im Neuenheimer Feld, 368, 69120 , Deutschland
Tel: +49-711-6862504, Fax: +49-711-6862578, E-Mail: jens.marquetand@iwr.uni-heidelberg.de

Prof. Dr. Uwe Riedel: Institut für Verbrennungstechnik, Deutsches Zentrum für Luft- und Raumfahrt (DLR), Pfaffenwaldring, 38-40, 70569 , Deutschland
Tel: +49-711-6862351, Fax: +49-711-6862578, E-Mail: uwe.riedel@dlr.de

Keywords: soot, modeling

MS-ID:

jens.marquetand@iwr.uni-heidelberg.de

October 22, 2010

Heft: / ()

Abstract

An existing two-equation soot model is extended by nucleation of soot particles from phenyl to improve the model's results for aromatic fuels. The model describes the soot formation processes by rate equations for the soot concentration and the soot volume fraction. These two equations are solved fully coupled with the rate equations of the gas-phase species resulting from a detailed chemical kinetics model.

The soot model is tested under shock-tube conditions for the oxidation of n-heptane and toluene. The maximum volume fraction needed as input to the two-equation model is derived from simulations with a detailed soot model, when no experimental values are given. Therefore a bell-shaped curve is fit to the detailed simulation's results and the so determined fit parameters are passed to the two-equation model.

Two sets of parameters for the simplified model are found, one representing the former version of the model with nucleation solely depending on propargyl and another one additionally including phenyl in the nucleation process. Both parameter sets show good agreement to the experimental values and nearly equal results for the time evolution and temperature dependence during the oxidation of n-heptane. However, during the oxidation of toluene additionally considering particle nucleation from phenyl improves the results compared to the former version of the two-equation model as the soot yield is predicted much better for lower temperatures.

1 Introduction

The public interest for the emissions of combustion devices increased a lot within the last years as they are made responsible for environmental and health problems. Besides CO, CO₂ and NO_x found in combustion exhaust gases the soot particle emission is of special interest, as it was found out to cause serious health defects like lung cancer. Therefore, the reduction of the soot particle emission is the most important aim in current soot formation research. Another aspect is the understanding of the soot formation itself. This is important for a deeper insight in the combustion processes as soot is playing an important role in the heat transfer of burners and furnaces and also can cause material damages in gas turbines, for example.

The formation of soot can be described in different steps: At the onset, there is the build-up of the first aromatic ring from species in the gas phase, such as acetylene and propargyl [1]. These smaller hydrocarbon result from decomposing the fuel molecules. The ring formation is regarded as a rate-limiting step in the evolution of soot particles [2]. These processes happening in the gas phase are described by elementary reactions.

The first aromatic ring gives rise to the build-up of polyaromatic hydrocarbons (PAHs): The number of rings increases by reactions with gas-phase species, mainly the ones mentioned above [1]. Further growth of the PAHs via joining and ongoing formation of aromatic rings finally leads to the build-up of soot particles [1].

The size of these primary particles increases when mainly acetylene from the gas phase reacts with their respective surfaces [1]. Another effect leading to larger soot particles is the coagulation of two particles [1], theoretically described by the Smoluchowsky equation [3].

Spurred by political and public interest there was big progress in research on the soot formation processes over the last years, both experimentally and theoretically. Despite all these progresses, also in the numerical simulations, the detailed simulation of the soot formation processes within models of multidimensional combustion systems is still prohibitive. Therefore, a reduced soot model like the two-equation model presented in this work is needed for implementation of soot formation and soot oxidation in CFD simulations. This model is based on the work of Moss [4], Sojka [5], and Naydenova [6] and was extended to give better results for aromatic fuels like toluene.

2 Model description

2.1 Detailed Kinetical Model

In this work a recently-developed kinetical model [6] is used for the simulation of the chemical reactions. It is based on previous work [7, 8] that combined a number of models for PAH formation and growth, soot particle nucleation, and the HACA reactions for PAH and soot particle growth from the literature, which was extended by several PAH formation and growth pathways up to seven aromatic rings [9].

Within the kinetics model the reactions happening during soot formation are formulated in two separate parts. The first one describes the reactions happening in the gas phase like the formation of the first aromatic ring from small hydrocarbons and the growth and formation of PAHs up to seven rings. As a combination of the submodels mentioned above this leads to 2094 elementary reactions (929 reversible, 198 irreversible Arrhenius-type, and 38 Troe-type reactions) among 199 species.

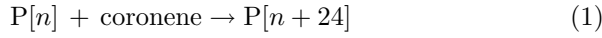
The second part of the kinetical model describes the transition of the gas-phase species to particulate matter and the growth of the soot particles. The nucleation of the soot precursors mainly happens in reactions involving PAHs and their radicals. The additional PAHs [9] mentioned above also contribute to the formation of the precursors. So new reactions for these PAHs are implemented in the kinetical model. Besides these changes concerning the precursor formation the second part of the kinetical model describing the growth and oxidation of the particles was not modified compared to [8]. The soot precursors and particles in the model are considered as large molecules dispersed in the gas phase. They are treated as polymer species permitting the formulation of elementary reactions for polymers similar to those applied for the gas-phase species. There are 105 polymer reactions between four polymer species and species from the gas phase included in the kinetical model. The polymer species represent the soot precursors, the soot particles and activated variants of both possessing radical sites.

The equations of the polymer species are solved with a discrete compartment method approach [10] which combines aspects of sectional and moment methods for population balance equations. Within the compartment method the particle size axis of the population balance is split into a given number of discrete intervals, the compartments i respectively. Inside these compartments the conservation equations for aggregated particle number and mass of every species are solved. These quantities correspond to the zeroth and first moments ($\mu_{P,0}^i, \mu_{P,1}^i$) of the polymer species P.

In this work a single compartment is used ranging over the whole size distribution resulting in the total moments $\mu_{P,0}, \mu_{P,1}$ of the species. This formulation results in neglecting size-dependent kinetic effects. The implementation of the compartment model with the four polymer species

in the kinetical model leads to eight additional equations, two per species and interval.

The rate equations of the moments $\mu_{P,0}, \mu_{P,1}$ for a single compartment are essentially as simple as the rate equations for the gas-phase species. E.g., for the growth of soot precursor particles by coronene, having 24 carbon atoms, the polymer reaction scheme is



with n representing the number of C-atoms, the monomers used in the compartment model. The respective contributions to the rates, assuming a kinetic coefficient k , are:

$$\frac{dC_{\text{coronene}}}{dt} = -k \cdot \mu_{P,0} \cdot C_{\text{coronene}} \quad (2)$$

for the coronene concentration C_{coronene} , and

$$\frac{d\mu_{P,0}}{dt} = k \cdot \mu_{P,0} \cdot C_{\text{coronene}} \quad (3)$$

$$\frac{d\mu_{P,1}}{dt} = 24 \cdot k \cdot \mu_{P,0} \cdot C_{\text{coronene}} \quad (4)$$

for the moments of polymer species P .

For calculations with the simplified two-equation model, updates to the hydrocarbon reactions from C_1 to C_4 were made following literature recommendations for the rate coefficients [11]. This modification increased the number of species in the gas-phase part of the kinetical model to 213 and 2379 reactions in this version.

2.2 Two-equation soot model

The exact formation process of soot is hardly understood as described above. There are numerous interacting reactions and processes happening while a particle is formed and growing from species in the gas phase. In this model all these reactions are grouped into four main processes: nucleation, coagulation, surface growth, and oxidation.

Nucleation describes the formation of the so-called primary particles, which consist of PAHs that are formed by species reacting in the gas-phase. In the current model propargyl and phenyl are representing the nucleation process. Both are known to play an important role in the formation of the first aromatic ring and its growth [1], but they also show the temperature dependence needed for the nucleation in the model to correspond with experiments. At high temperatures and in aliphatic fuels the nucleation in the model depends on propargyl, whereas phenyl is responsible for nucleation mostly in aromatic fuels and at lower temperatures.

Coagulation happens, when two soot particles collide with each other and stick together forming a larger particle. This decreases the number

of particles in the system, thus reduces the soot concentration, but does not affect the soot volume fraction at all.

The surface growth process describes the reaction of gas-phase species with the surface of a soot particle, thereby increasing the volume of the particle. The particles in the model are considered spherical, following a commonly used assumption. As suggested in literature, the species contributing most to surface growth is acetylene [12]. Therefore, this process is implemented depending on the concentration of acetylene.

Instead of increasing the volume of the particles it is decreased by oxidation. Here OH is assumed to be the dominant species reacting with the particle surface.

The soot formation processes described above are represented here by two rate equations: One considering the soot concentration which gives an information of the number of particles (Eq. (5)). The other one, the rate equation of the soot volume fraction, corresponding to the volume or the mass, respectively (Eq. (6)).

The nucleation and coagulation both influence the number of particles and therefore are part of the soot concentration rate equation

$$\frac{dC_{\text{soot}}}{dt} = \underbrace{\alpha_1 \cdot C_{\text{C}_3\text{H}_3}^2 + \alpha_2 \cdot C_{\text{C}_6\text{H}_5}^2}_{\text{nucleation } \tilde{\alpha}_1, \tilde{\alpha}_2} - \underbrace{\beta \cdot C_{\text{soot}}^2}_{\text{coagulation}}. \quad (5)$$

As mentioned already nucleation in the model is depending on the species concentrations of propargyl and phenyl. The parameters α_1 and α_2 in the nucleation part of Eq. (5) represent the different contributions of the respective species to the nucleation of the soot particles. The representation of the complicated particle nucleation from the gas phase depending on just two species concentrations is a strong simplification of the real processes. Therefore it is not possible to determine the values of the parameters α_1 and α_2 directly from theory. In this work these values are adjusted to represent the experimental results.

The coagulation depends on the soot concentration itself and the collision number β corresponding to the reaction of two soot particles with each other [13].

The rate equation of the soot volume fraction depends on nucleation, the surface growth and the oxidation, as these influence the volume of the

particles as formulated in

$$\begin{aligned} \frac{df_V}{dt} = & \underbrace{\delta_1 \cdot C_{C_3H_3}^2 + \delta_2 \cdot C_{C_6H_5}^2}_{\text{nucleation}} \\ & + \underbrace{\gamma \cdot C_{C_2H_2} \cdot C_{soot}^{1/3} f_V^{2/3} \left(1 - \frac{f_V}{f_{V,\infty}}\right)}_{\text{surface growth } \tilde{\gamma}} \\ & - \underbrace{\varepsilon \cdot C_{OH} \cdot C_{soot}^{1/3} f_V^{2/3}}_{\text{oxidation } \tilde{\varepsilon}}. \end{aligned} \quad (6)$$

δ_1 and δ_2 represent the contribution of the propargyl and phenyl to the nucleation, as described for the soot concentration rate. But here the unit transformation

$$\delta_i = \alpha_i \cdot \frac{M_{soot}}{\rho_{soot}} \quad (7)$$

of the parameters is needed to represent the nucleation process in the volume fraction rate equation.

The density of soot is chosen as $\rho_{soot} = 1.86 \text{ g/cm}^3$ [14] and the mass of a nucleating particle is assumed to be ten-times the mass of a benzene molecule $M_{soot} = 781.2 \text{ g/mol}$.

The surface growth and oxidation terms are derived from the kinetic theory of gases assuming a first-order growth law, as suggested in the literature [13, 15]. The corresponding model parameters γ and ε represent characteristic properties like the mass of the gas-phase species C_2H_2 and OH .

The factor $1 - f_V/f_{V,\infty}$ in Eq. (6) limits the contribution of the surface growth to an upper empirical value, the maximum volume fraction $f_{V,\infty}$, which can be measured experimentally. As $f_{V,\infty}$ is only given for a few experiments, values resulting from simulations with the detailed soot model were used. To represent the temperature dependence of these values within the simplified model the Eq. (8) is used which by adjusting the parameters a_i and b_i is fit to the bell-shaped results of the detailed model.

$$f_{V,\infty}^{fit}(T) = \frac{a_1}{a_2} \cdot \exp\left(\frac{-(T - a_3)^2}{a_2}\right) + \frac{b_1}{b_2} \cdot \exp\left(\frac{-(T - b_3)^2}{b_2}\right), \quad (8)$$

For some detailed simulations a single bell-shaped curve is not representing the temperature dependence of $f_{V,\infty}$. In these cases the second bell-shaped curve is considered additionally by using parameters $b_i \neq 0$.

The particle diameter D_{soot} is calculated with the soot concentration and the volume fraction resulting from the source terms of Eqs. (5) and (6). As spherical particles are assumed, the diameter can be calculated as

$$D_{soot} = \left(\frac{6 \cdot f_V}{\pi \cdot C_{soot} \cdot N_A}\right)^{1/3} \quad (9)$$

with N_A representing Avogadro's number.

The soot yield Y_{soot} , the fraction of carbon transformed to soot, is calculated as

$$Y_{\text{soot}} = \frac{C_{\text{C,soot}}}{C_{\text{C,total}}}. \quad (10)$$

Here, $C_{\text{C,total}}$ stands for the total carbon atom concentration in the system and is determined by the initial concentration of the fuel and the number of carbon atoms within. $C_{\text{C,soot}}$ represents the concentration of C-atoms appearing in the soot particles which is calculated from

$$C_{\text{C,soot}} = \frac{N_A \cdot f_V \cdot \rho_{\text{soot}}}{M_C} \quad (11)$$

where M_C is the molar mass of a C-atom.

The concentrations of the gas-phase species (C_2H_2 , C_3H_3 , C_6H_5 , OH) used in the two-equation soot model are calculated using the gas-phase part of the detailed kinetic model (see Section 2.1). The feedback from the simplified soot model back to the detailed gas phase chemistry is given by

$$\frac{dC_{\text{C}_3\text{H}_3}}{dt} = \left[\frac{dC_{\text{C}_3\text{H}_3}}{dt} \right]_{\text{gas}} - 2 \cdot \tilde{\alpha}_1 \quad (12)$$

$$\frac{dC_{\text{C}_6\text{H}_5}}{dt} = \left[\frac{dC_{\text{C}_6\text{H}_5}}{dt} \right]_{\text{gas}} - 2 \cdot \tilde{\alpha}_2 \quad (13)$$

$$\frac{dC_{\text{C}_2\text{H}_2}}{dt} = \left[\frac{dC_{\text{C}_2\text{H}_2}}{dt} \right]_{\text{gas}} - \tilde{\gamma} \frac{\rho_{\text{soot}}}{m_{\text{C}_2\text{H}_2} N_A} \quad (14)$$

$$\frac{dC_{\text{OH}}}{dt} = \left[\frac{dC_{\text{OH}}}{dt} \right]_{\text{gas}} - \tilde{\epsilon} \frac{\rho_{\text{soot}}}{m_{\text{OH}} N_A}. \quad (15)$$

The variables $\tilde{\alpha}_1$, $\tilde{\alpha}_2$, $\tilde{\gamma}$, and $\tilde{\epsilon}$ represent the rates of the processes nucleation, surface growth, and oxidation as formulated in Eqs. (5) and (6).

3 Results

The simulations shown here are carried out using the gas-phase reaction mechanism described in section 2.1. The two rate equations for the soot concentration and the soot volume fraction are implemented in a program for the simulation of a spatially homogeneous reaction system. They are solved fully coupled to the rate equations describing the concentration change of the gas-phase species using the DAE solver DASSL. At every integration step the results of the algebraic equations for the diameter and the soot yield are calculated, also.

The experimental values presented by Kellerer et al. [16] were determined with a refractive index given by Lee and Tien [17]. For consistency, those values are recalculated with the refractive index from Chang and

Charalampopoulos [18], which was used by Alexiou and Williams [19] for their toluene oxidation experiments. The newly resulting values are smaller by a factor of about two thirds, then the ones originally given by Kellerer et al. [16].

3.1 Maximum Volume Fraction

Although measurable in experiments the maximum volume fraction $f_{V,\infty}$ needed for the simplified soot model is rarely given in the literature. Regarding the experiments used for validation in this work neither Kellerer et al. [16] nor Alexiou and Williams [19] report this values. So for these experiments the value of $f_{V,\infty}$ needs to be derived from simulations with the detailed model to allow testing the simplified model with the experiments mentioned above.

These simulations are done at the same conditions as the experiments and the parameters of the bell shaped equation (8) are adjusted to fit the results. As an example the fit for the oxidation of n-heptane at 40 bar is shown in Fig. 1 together with the results from the detailed model.

There is a very good agreement between the simulation results and the fitted curve in this case. But, under some conditions there is only a poor fit when using just one bell-shaped curve. Therefore a second curve is applied additionally (see Eq. (8)) which leads to a very good agreement for those conditions, also. Figure 2 presents such a fit consisting of two curves together with the results from the detailed simulation of toluene oxidation with 1.5% oxygen.

The parameters a_i and b_i found by fitting to the results of the detailed model are passed to the simulation program with the simplified soot model via a data file. Within this program the value of $f_{V,\infty}$ is recalculated for the corresponding temperature.

Using the fit parameters representing the maximum volume fractions from the detailed simulations allows to do simulations with the two-equation model and to compare those with experiments providing the soot yield, only. The simulations with the detailed model need to be done only once. When the fit curve is known, no further simulations with the detailed model are needed. If the values of the maximum volume fraction are known from the experiments additional simulations with the detailed soot model are not necessary at all.

3.2 Oxidation of n-heptane

Two sets of parameters for the simplified soot model are found: parameter set A with nucleation solely depending on propargyl (see table 1) representing the simplified soot model as presented by Naydenova [6] and parameter set B additionally including nucleation from phenyl (see table 2). The kinetic parameters of α_2 in set B are chosen similar to the

ones of the reaction between two phenyl-radicals as given in the gas-phase mechanism described in section 2.1.

In Fig. 3 the results obtained with these two sets of parameters are compared with experiments [16] for the time evolution of the soot concentration, the particle diameter, and the soot yield during n-heptane rich-oxidation. A maximum volume fraction $f_{V,\infty} = 7.77 \cdot 10^{-6}$ is used, which is calculated from the soot concentration and particle diameter measured in the experiments, applying Eq. (10).

In the simulation, there is a faster increase of the soot concentration at the beginning than measured in the experiments. The reason is the direct dependence of the soot concentration on the propargyl- and phenyl-radical concentration. They both show the same characteristics: A rapid increase within the first 0.1 ms and a plateau at later reaction times (see Fig. 4). The maximum soot concentration is under-predicted during most of the simulation time, but at the end of the simulation time the concentration reaches the level of the experiments.

Within the the first millisecond the computed particle diameter is over-predicted which is a result of the under-predicted soot concentration in this phase of the simulation. When the soot concentration reaches the level of the experiments at the end of the simulation, the particle diameter is in good agreement with the measured values, also.

The computed soot yield is in very good agreement with the experiments. As soot yield in the model is depending directly on the volume fraction, one could state that also the volume fraction could be predicted correctly, if given in the experiments.

There is a very good agreement between the two sets of parameters for the simplified soot model with the parameter set including phenyl nucleation giving a slightly higher soot concentration and yield.

The feedback effects of the simplified soot model to the gas-phase species are given in Fig. 4 for simulations with parameter set B. Here the concentrations of the species implemented in the soot model are plotted as a function of time with and without the activation of the soot model in the simulation, thereby also considering the feedback of the model to the gas phase, or not. So the difference in the concentrations is a consequence of the feedback to the gas phase. Figure 4 also shows the concentrations of the soot precursors pyrene and coronene.

There is nearly no influence on the concentrations of C_3H_3 , C_6H_5 and OH whereas the concentration of C_2H_2 is lower throughout the whole reaction time, when the soot model is activated. As expected, the soot model also reduces the concentrations of the precursor species pyrene and coronene as the additional direct pathway to soot in the simplified model bypasses these species.

The temperature dependence of the soot yield for the oxidation of n-heptane is given in Fig. 5 for the simulations and the experiments [16]. The two parameter sets of the simplified model give the same results as they can not be distinguished in the plot. They both reproduce the

results of the simulations with the detailed model which are carried out for determination of the maximum volume fraction. All three models underpredict the maximum level of the soot yield, but the temperature of the maximum is predicted with a good agreement of about 50 K higher than measured.

3.3 Oxidation of toluene

The simplified soot model with additionally forming particles from phenyl is also tested for the oxidation of the aromatic toluene as the implementation of the model just using propargyl as a nucleation species is not well predicting the soot yield under these conditions. The simulated results of the soot yield for toluene with different mole fractions of oxygen are given in Fig. 6 together with the measured values [19].

While there is no big difference between the detailed and the simplified model for the aliphatic fuel n-heptane here, there is a big deviation between both and also the results with or without phenyl contributing to nucleation differ significantly. The detailed model overpredicts the soot yield by far for the oxidation, but correctly represents pyrolysis. There is no difference in the temperature maximum of the soot yield with the detailed model but the maximum temperature decreases with the simplified model when adding oxygen, as measured in the experiments. Additionally implementing nucleation from phenyl in the simplified model shifts the maximum temperature closer to the experimental values and also improves the model prediction for temperatures lower than 1800 K. Although the level of the soot yield is well predicted for the oxidative conditions now, the simplified model still underpredicts the level at pyrolysis.

4 Conclusion

An existing two-equation soot model [6] showing weaknesses with aromatic fuels is extended. The model presented here additionally incorporates nucleation of soot particles from phenyl and also has the capability of a variable maximum soot volume fractions $f_{V,\infty}$ depending on the temperature.

Due to the lack of experimental data the values of $f_{V,\infty}$ are obtained from simulations using a detailed soot model [6, 10]. The parameters of a bell-shaped curve are fit to the results of the detailed model and subsequently passed to the simplified model via a data file. Once the fit curve is known for the observed conditions, no further simulations with the detailed soot model are needed.

Parameters for the fit curve are determined for the oxidation of n-heptane at different pressures from 30 bar to 50 bar and for the oxidation of toluene with different mole fractions of oxygen. The parameters found

are used for calculating the maximum volume fraction within simulations with the two-equation model.

The two-equation soot model is applied for the oxidation of n-heptane and toluene. Two parameter sets for the simplified model are found, one considering the nucleation only depending on propargyl as in the former version of the model, the other one additionally including nucleation from phenyl. The model results are compared with the time evolution of the soot concentration, particle diameter and soot yield measured during the oxidation of n-heptane [16]. A good agreement is found for both parameter sets under these conditions, especially the soot yield is well represented by the model.

The effect of the soot model on the concentrations of the gas-phase species shows the expected results with lowering the concentrations of the soot precursors in the gas phase.

Comparing the model results with the experimental temperature dependence of the soot yield during the oxidation of n-heptane [16] shows good agreement. The results of the simplified model just slightly differs from the ones obtained with the detailed model.

The results for the oxidation of toluene improves when activating the nucleation of phenyl in the simplified model. The temperature maximum of the soot yield shifts to lower temperatures and soot yield at temperatures up to 1800 K is predicted much better. For oxidation of toluene the prediction of the simplified soot model is closer to experiments than the detailed one, which gives good results just for pyrolysis conditions.

Acknowledgments

The financial support of the “Deutsche Forschungsgemeinschaft” (German Research Foundation) within the Collaborative Research Center 568 is gratefully acknowledged.

References

- [1] M. Frenklach, Phys. Chem. Chem. Phys. **4** (2002) 2028.
- [2] H. Wang and M. Frenklach, Combust. Flame **110** (1997) 173.
- [3] M. von Smoluchowski, Ritter von Smolan, Z. Phys. Chem. **92** (1917) 129.
- [4] J. B. Moss, C. D. Stewart, and K. J. Young, Combust. Flame **101** (1995) 491.
- [5] J. Sojka, *Simulation der Rußbildung unter homogenen Verbrennungsbedingungen*, Ph.D. thesis, Ruprecht-Karls-Universität Heidelberg (2001).

- [6] I. Naydenova, *Soot formation modeling during hydrocarbon pyrolysis and oxidation behind shock waves*, Ph.D. thesis, Ruprecht-Karls-Universität Heidelberg (2007).
- [7] P. A. Vlasov and J. Warnatz, *Proc. Comb. Inst.* **29** (2002) 2335.
- [8] G. L. Agafonov, I. Naydenova, P. A. Vlasov, and J. Warnatz, *Proc. Comb. Inst.* **31** (2007) 575.
- [9] H. Richter, S. Granata, W. H. Green, and J. B. Howard, *Proc. Comb. Inst.* **30** (2005) 1397.
- [10] M. Nullmeier, *A Discrete Compartment Method for Soot Polymerization Kinetics*, Ph.D. thesis, Ruprecht-Karls-Universität Heidelberg (in preparation).
- [11] D. Baulch, C. Bowman, C. Cobos, R. Cox, T. Just, J. Kerr, M. Pilling, D. Stocker, J. Troe, W. Tsang, R. Walker, and J. Warnatz, *J. Phys. Chem. Ref. Data* **34** (2005) 757.
- [12] M. Frenklach and H. Wang, *Soot Formation in Combustion*, chapter Detailed mechanism and kinetic modeling of soot particle formation, Springer-Verlag, Berlin, Heidelberg (1994), 162–190.
- [13] B. S. Haynes and H. G. Wagner, *Prog. Energy Combust. Sci.* **7** (1981) 229.
- [14] S. Graham, J. Homer, and J. Rosenfeld, *Proc. R. Soc. London, Ser. A* **344** (1975) 259.
- [15] P. W. Atkins, *Physical chemistry*, Oxford University Press, New York, 7th edition (2002).
- [16] H. Kellerer, A. Müller, H.-J. Bauer, and S. Wittig, *Combust. Sci. Technol.* **113-114** (1996) 67.
- [17] S. C. Lee and C. L. Tien, *Proc. Comb. Inst.* **18th** (1981) 1159.
- [18] H. Chang and T. T. Charalampopoulos, *Proceedings of the Royal Society: Mathematical and Physical Sciences (1990-1995)* **430** (1990) 577.
- [19] A. Alexiou and A. Williams, *Combust. Flame* **104** (1996) 51.

Table 1: Parameter set A, parameters of the two-equation model without phenyl contributing to nucleation

α_1	$6.0 \cdot 10^3$	$\frac{\text{m}^3}{\text{mol}\cdot\text{s}}$
α_2	0.0	$\frac{\text{m}^3}{\text{mol}\cdot\text{s}}$
β	$1.0 \cdot 10^9 \cdot T^{1/2}$	$\frac{\text{m}^3}{\text{mol}\cdot\text{s}\cdot\text{K}^{1/2}}$
γ	$99.82 \cdot T^{1/2}$	$\frac{\text{m}^4}{\text{mol}\cdot\text{s}\cdot\text{K}^{1/2}}$
ϵ	$3.34 \cdot 10^3 \cdot T^{1/2}$	$\frac{\text{m}^4}{\text{mol}\cdot\text{s}\cdot\text{K}^{1/2}}$

Table 2: Parameter set B, parameters of the two-equation model with phenyl contributing to nucleation

α_1	$5.0 \cdot 10^3$	$\frac{\text{m}^3}{\text{mol}\cdot\text{s}}$
α_2	$2.0 \cdot 10^{13} \cdot T^{1/2} \cdot \exp\left(\frac{12133}{RT}\right)$	$\frac{\text{m}^3}{\text{mol}\cdot\text{s}}$
β	$1.0 \cdot 10^9 \cdot T^{1/2}$	$\frac{\text{m}^3}{\text{mol}\cdot\text{s}\cdot\text{K}^{1/2}}$
γ	$99.82 \cdot T^{1/2}$	$\frac{\text{m}^4}{\text{mol}\cdot\text{s}\cdot\text{K}^{1/2}}$
ϵ	$3.34 \cdot 10^3 \cdot T^{1/2}$	$\frac{\text{m}^4}{\text{mol}\cdot\text{s}\cdot\text{K}^{1/2}}$

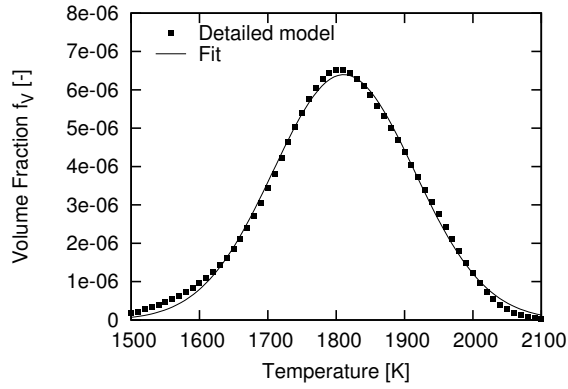


Figure 1: Function (8) fit to the volume fractions resulting from the detailed soot model for the oxidation of n-heptane with oxygen in argon ($x_{\text{Ar}} = 99\%$, $\Phi = 5$, $p = 40$ bar, $\tau_{\text{sim}} = 2.0$ ms) by adjusting the parameters a_i .

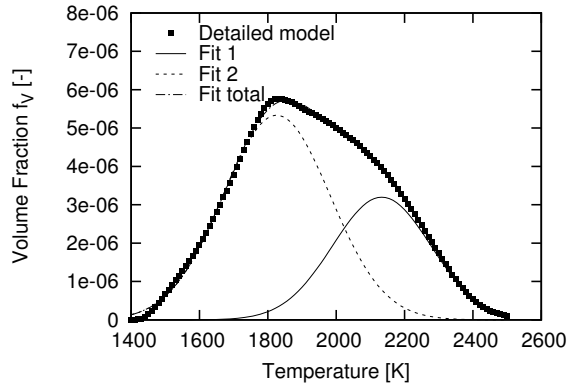


Figure 2: Function (8) fit to the volume fractions resulting from the detailed soot model for the oxidation of toluene with oxygen in argon ($x_{\text{toluene}} = 1.5\%$, $x_{\text{O}_2} = 1.5\%$, $p = 2.48$ bar, $\tau_{\text{sim}} = 2.0$ ms) by adjusting the parameters a_i and b_i .

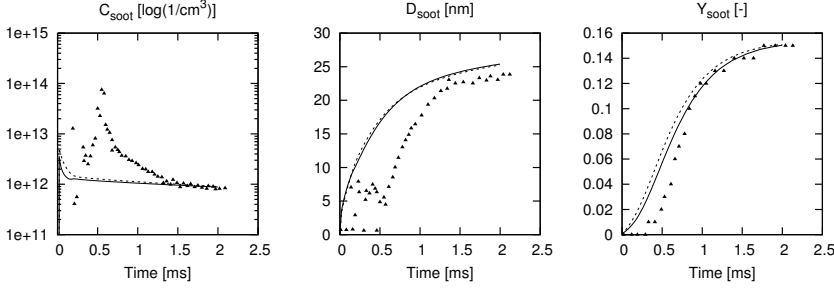


Figure 3: Time-resolved soot concentration, particle diameter, and soot yield, measured ([16], symbols) and calculated (lines), during $n\text{-C}_7\text{H}_{16}$ rich-oxidation without (solid) and with phenyl (dashed) contributing to nucleation ($[\text{C}] = 7.89 \text{ mol/m}^3$, $\Phi = 5$, $T = 1750 \text{ K}$, $p = 25 \text{ bar}$, $\tau_{\text{sim}} = 2.0 \text{ ms}$).

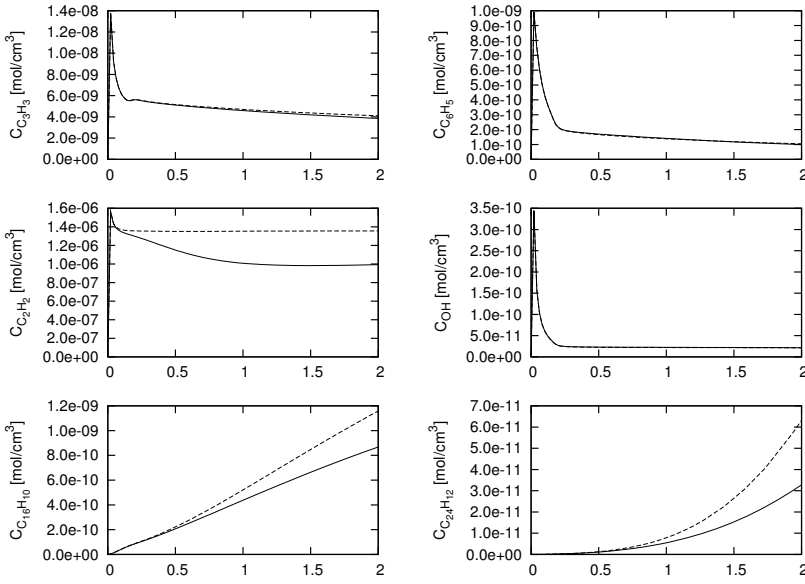


Figure 4: Time-resolved concentrations of species implemented in the simplified soot model and influence of the soot model on the concentrations of some soot precursor species during $n\text{-C}_7\text{H}_{16}$ rich-oxidation ($[\text{C}] = 7.89 \text{ mol/m}^3$, $\Phi = 5$, $T = 1750 \text{ K}$, $p = 25 \text{ bar}$, $\tau_{\text{sim}} = 2.0 \text{ ms}$, [16]) with (solid) and without (dashed) activation of the soot model including phenyl. Parameters for the simplified soot model as given in table 2.

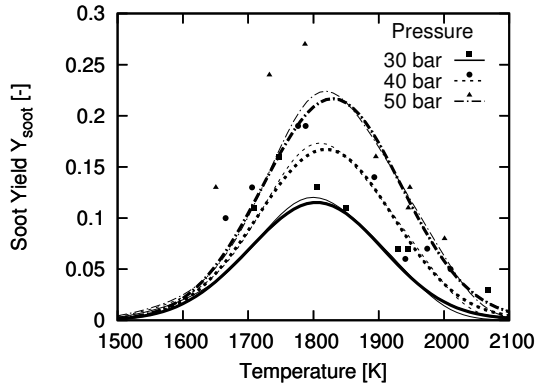


Figure 5: Soot yield for the oxidation of n-heptane with oxygen in argon at different pressures ($x_{\text{Ar}} = 99\%$, $\Phi = 5$, $\tau_{\text{sim}} = 2.0$ ms) experimental (symbols) and simulated (lines) with the detailed (thin) and the simplified model without (medium), and with (thick) phenyl contributing to nucleation.

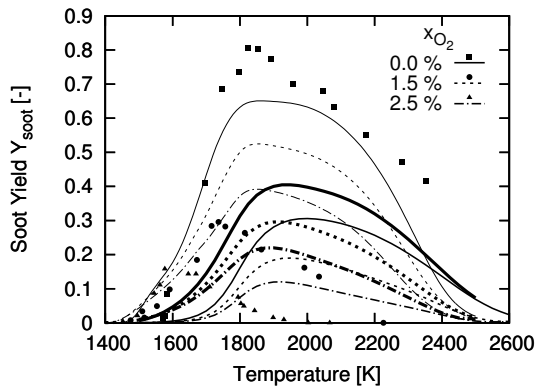


Figure 6: Soot yield for the oxidation of toluene with oxygen at different mole fractions in argon ($x_{\text{toluene}} = 1.5\%$, $\tau_{\text{sim}} = 2.0$ ms) experimental (symbols) and simulated (lines) with the detailed (thin) and the simplified model, without (medium), and with (thick) phenyl contributing to nucleation.